HYPERFILTRATION-INDUCED PRECIPITATION OF SODIUM CHLORIDE

By

T. M. Whitworth[1]
Principal Investigator
NMBMMR
New Mexico Tech

and

Chen Gu
Research Assistant
Department of Environmental Engineering
New Mexico Tech

TECHNICAL COMPLETION REPORT

Account Number 01423959

February, 2001

New Mexico Water Resources Research Institute

In cooperation with

New Mexico Bureau of Mines and Mineral Resources

And

Department of Environmental Engineering
New Mexico Tech

---

[1] Now at the University of Missouri-Rolla, Department of Geological and Petroleum Engineering, Rolla, MO.

DISCLAIMER

The purpose of the Water Resources Research Institute technical reports is to provide a timely outlet for research results obtained on projects supported in whole or in part by the institute. Through these reports we are promoting the free exchange of information and ideas, and hope to stimulate thoughtful discussions and actions which may lead to resolution of water problems. The WRRI, through peer review of draft reports, attempts to substantiate the accuracy of information contained in its reports, but the views expressed are those of the authors and do not necessarily reflect those of the WRRI or its reviewers. Contents of this publication do not necessarily reflect the views and policies of the Department of the Interior, nor does the mention of trade names or commercial products constitute their endorsement by the United States government.

ACKNOWLEDGMENTS

ABSTRACT

In a previous WRRI-funded project (Whitworth and DeRosa 1997), heavy metals including copper, cobalt, and lead, were successfully precipitated from initially undersaturated chloride solutions forced through clay membranes (hyperfiltration). Those metal chlorides are quite soluble, but not as soluble as sodium chloride, a common constituent of almost all waters. However, theoretical calculations suggested that it is not only possible to precipitate sodium chloride from an initially undersaturated solution passing through a clay membrane, but that it can be done at fluid pressures of less than 400 psi—pressures significantly less than those used in most reverse osmosis systems. Therefore, we tested the concept that clay membranes can concentrate and precipitate NaCl in a series of hyperfiltration experiments. Some of the experiments resulted in formation of sodium chloride crystals on the surface of the membrane when undersaturated NaCl solutions were forced through the membranes. We used both bentonite and kaolinite clay membranes in these experiments. We discovered in the early experiments, that ethanol, which is commonly used to displace water, forms an azeotrope when mixed with water and this results in NaCl precipitation when the NaCl concentrations are high enough. To avoid this problem, we displaced the water in the experimental cells and membranes with cooking oil before examining the clay membranes for the presence of NaCl crystals. Consequently, we did observe NaCl precipitation when undersaturated solutions were passed through both kaolinite and bentonite membranes. Thus, the initial concept appears to be valid. Further work will be required to develop this into a commercial application.

TABLE OF CONTENTS

LIST OF FIGURES

LIST OF TABLES

JUSTIFICATION OF WORK PERFORMED

Less than two percent of the world's water is fresh water suitable for drinking (Fetter 1988). The rest is too saline for human consumption (i. e., total dissolved solids greater than 1000 mg/l). Therefore, as world population grows, especially in arid or semiarid areas, fresh water supplies are often being consumed faster than they can be naturally replaced. This is currently the situation in the city of Albuquerque, where groundwater levels are dropping every year and conservation measures are being implemented. It is increasingly important that cost-effective methods be developed for use of saline or other impaired waters in order to ensure adequate future water supplies for the people of the state of New Mexico as well as the rest of the world.

Large volumes of saline waters underlie about two-thirds of the continental United States, including New Mexico (Feth 1970). Few aquifers in New Mexico contain only fresh water. Most also contain significant volumes of saline water, often at relatively shallow depths (Hood and Kister 1962).

Conventional reverse osmosis shows promise of providing an economical method of purifying saline and other impaired waters. However, a major limitation is its relatively large waste stream. For some applications this waste stream can be as much as 80% of the total volume treated. High waste disposal costs rule out or severely limit the use of reverse osmosis for many applications. The goal of this project is to investigate a process that shows promise of being able to reduce that waste stream to a solid—a reduction in waste volume of up to four orders of magnitude—thus allowing all of the water input into the system to be purified. In a previous WRRI-funded project (Whitworth and DeRosa 1997), we successfully precipitated heavy metals including copper, cobalt, and lead, from undersaturated chloride solutions passed through clay[2] membranes. Metal chlorides, such as $CuCl_2$, $PbCl_2$, and $CoCl_2$, are quite soluble (with solubilities ranging from 5.7×10^{-5} to 3.47 molar), but not as soluble as sodium chloride (solubility 6.2 molar). Sodium chloride is the most common constituent of saline waters and is the only constituent of natural waters in which concentrations commonly exceed 20,000 mg/l (Feth 1970).

If a reverse osmosis waste reduction system is to be widely applicable, it must be able to precipitate highly soluble dissolved minerals such as sodium chloride as well as less soluble dissolved minerals. Theoretical calculations suggest that, it is not only possible to precipitate sodium chloride from an initially undersaturated solution passing through a membrane, but that it can be done at fluid pressures of less than 400 psi—pressures significantly less than those used in most reverse osmosis systems. The calculations follow in a later section.

The secret to hyperfiltration-induced precipitation of highly soluble minerals such as sodium chloride at such low pressures is through the use of an osmotically inefficient membrane. Clay membranes will be used in the experiments because their osmotic efficiency is related to the amount of compaction, which is simple to control in the experiments.

DESCRIPTION OF HYPERFILTRATION EFFECTS

Osmotic pressure is generated when a membrane separates solutions of differing concentrations. Water will diffuse through the membrane into the reservoir with the higher solute concentration, thus increasing the pressure in that reservoir. The equilibrium pressure in the reservoir with the higher solute concentration is called the effective osmotic pressure. Some solute will also leave the high solute concentration reservoir, diffuse through the membrane, and enter the lower solute concentration reservoir. Hyperfiltration (also called reverse osmosis) occurs when pressure in excess of osmotic is applied to the membrane and the water flux is forced to reverse direction. Some solute is then rejected by the membrane and accumulates on the higher-pressure side of the membrane. Conventional cross-flow reverse osmosis units prevent this solute build up by sweeping the high pressure membrane face with a turbulent, high-velocity flux.

When the solute is not swept away and is allowed to build up, hyperfiltration begins with identical solute concentrations on both sides of the membrane at time t = 0 (Fig. 1a). Because water

---

[2] Montmorillonite is the clay mineral used in these experiments. It is also commonly referred to by the group names bentonite or smectite.

passes more easily through the membrane than solute, the solute begins to accumulate at the high-pressure

membrane face (Fig. 1b). The zone of increased concentration is called the concentration polarization

layer (CPL). As the CPL grows, ever more solute is available at the high-pressure membrane face to

enter the membrane. Hence, membrane efficiency decreases and effluent concentration tends to increase

concurrently with CPL growth (Fritz and Marine 1983). The concentration at the high-pressure

membrane face continues to increase over time as does the width and mass of solute in the CPL (Fig. 1c).

Eventually, if no precipitation or chemical reaction occurs, an equilibrium is reached (Fig. 1d) in which

the effluent concentration stabilizes at that of the original input concentration. However, concentrations

within this CPL can easily reach saturation and/or supersaturation, which results in solute precipitation.

When precipitation occurs, the system will reach a steady state in which the effluent concentration is less

than the input concentration. It is the equilibrium state in which continuous precipitation occurs that is

the objective of the experiments.

Membrane Mathematics

        Kedem and Katchalsky (1962) derived two equations that describe the flow of solution and solute

through membranes. These equations were developed for non-electrolytes, but have been successfully

applied to electrolytes (Spiegler and Kedem 1966; Harris et al. 1976; Mariñas and Selleck 1992;

Whitworth et al. 1994). They describe a conservative, single solute system. The two equations are:

$$J_v = L_p(\Delta P - \sigma \Delta \pi) \tag{1}$$

    and

$$J_s = \bar{c}_s(1-\sigma)J_v + \omega \Delta \pi \tag{2}$$

Where J_v = solution flux (cm/s) through the membrane, L_p = water permeation coefficient (cm^3/dyne·s),

ΔP = pressure difference across the membrane (dyne/cm^2), σ = reflection coefficient (dimensionless), $\Delta \pi$

= theoretical osmotic pressure difference across the membrane (dyne/cm^2), J_s = solute flux (mole/cm^2·s)

3

through the membrane, ω = solute permeation coefficient (mole/dyne·s), and $\bar{c}_s$ = average solute

concentration across the membrane in mole/cm^3 where
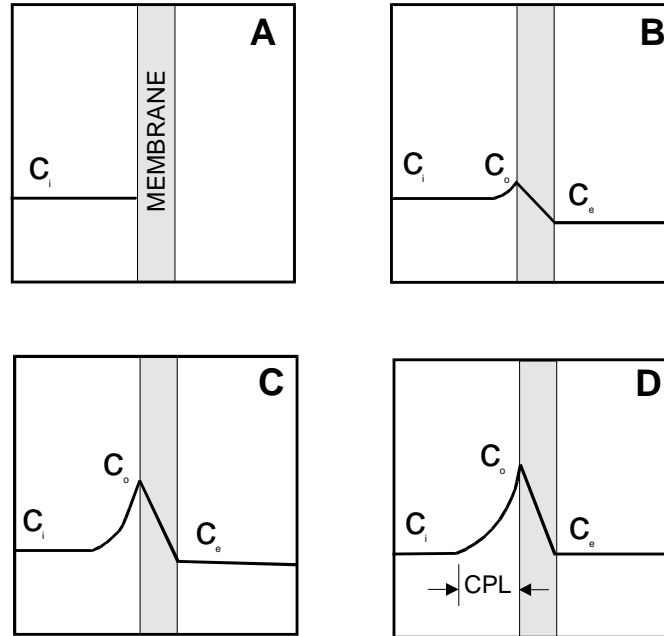
Figure 1. Conceptual development of a concentration polarization layer. The initial conditions (A) are such that the solute is all on the high pressure side of the membrane and the pore fluids within the membrane contain no solute. Some time after solute flux through the membrane begins (B) the concentration at the high pressure membrane face c_o increases because some of the solute is rejected by the membrane. Some solute also begins to pass through the membrane so that the effluent now contains some solute as well. Even later (C) c_o has increased further as has the effluent concentration c_e. At steady-state (D), where no precipitation or chemical reactions are occurring, the input concentration c_i is now equal to c_e and the value of c_o is constant. If saturation is reached or exceeded in the CPL and precipitation occurs, an equilibrium is reached in which $c_e < c_o$, similar to C (Redrawn from Fritz and Marine 1983).

$$\bar{c}_s = \frac{c_o + c_e}{2} \tag{3}$$

where c_o = concentration at the high-pressure membrane face (mole/cm^3) and c_e = effluent concentration

(mole/cm^3).

The equation for $\Delta\pi$ for a dilute single solute is

$$\Delta\pi = vRT(c_o - c_e) \tag{4}$$

Where v is a factor that corrects for the number of particles due to ion formation. For example, since NaCl forms two ions in solution, Na^+ and Cl^-, then for NaCl, v = 2. However, for $CaCl_2$, which forms one Ca^{++} ion and two Cl^- ions for each molecule of $CaCl_2$, v = 3. In Equation 3, R is the gas constant (8.314×10^7 dyne·cm/mole·°K) and T is the temperature in °K.

Fritz (1986) suggested that three of the phenomenological coefficients of Kedem and Katchalsky (1962)—σ, ω, and L_p —are useful in describing the behavior of non-ideal, clay membrane systems. First, consider the reflection coefficient σ. Permissible values of σ range from zero to one. If $\sigma = 0$, then there is no membrane effect. In this case Equation 1 reduces to a one-dimensional form of Darcy's Law. If $\sigma = 1$, the membrane is ideal and no solute can pass. The value of σ for non-ideal clay membranes must be greater than zero, but less than one. Fritz and Marine (1983) calculated values of σ for a series of six experiments using montmorillonite clay membranes compacted to different porosities and NaCl solutions. The values of σ they determined ranged from 0.04 to 0.89. Fritz and Marine (1983) state that σ is important because it is a measure of osmotic efficiency. Thus, a membrane with a $\sigma = 0.90$ would exhibit 90% of the theoretically predicted osmotic pressure. For solutes such as NaCl, with identical anion and cation concentrations, $\sigma_{anion} = \sigma_{cation}$. However, for systems such as $CuCl_2$, where the dissolved anion concentration is twice that of the cation concentration, the anion and the cation have differing values of σ.

The solute permeation coefficient ω describes the diffusion of solute through the membrane. For ideal membranes, $\omega = 0$ and no solute can pass through the membrane. For typically non-ideal clay membranes ω should be greater than zero. Elrick et al. (1976) measured ω for a Na-montmorillonite slurry with 90% porosity and obtained a value of 3×10^{-15} mole/dyne·s. Fritz and Marine (1983) suggested that for more compacted clays, the value of ω should be considerably lower than 3×10^{-15} mole/dyne·s. For systems where the anion concentration is not equal to the cation concentration, $\omega_{anion} \neq \omega_{cation}$.

The water permeation coefficient L_p is related to the hydraulic conductivity K (in cm/s) by the expression (Fritz 1986)

$$L_p = \frac{K}{\rho g \Delta x}$$

(5)

where ρ is the fluid density in g/cm^3, g is the gravitational constant in cm/s^2, and Δx is the membrane thickness in cm. In general, as L_p decreases, membrane efficiency increases (Fritz 1986).

Fritz and Marine (1983) derived a steady-state solution that describes the concentration profile within the free solution abutting the membrane. Their equation is

$$c_x = (c_o - c_i)\left[\exp(\frac{-J_v x}{D}) - \exp(\frac{-J_v x_i}{D})\right] + c_i$$

(6)

Where c_x is the concentration in moles/cm^3 at distance x (cm) from the membrane, and x_i is the distance from the membrane where $c_x = c_i$. In Equation 6, J_v represents the flux toward the membrane. Fritz and Whitworth (1994) state that the term $-\exp(-J_v x_i/D)$ in Equation 6 can be ignored if the length of the test cell is large relative to the ratio D/J_v.

Derivation

In order to use Equation 6 to model the proposed experiments, c_o must be known. An analytical expression for c_o can be derived by substituting Equations 3, 4, 5, the following expression for ω

$$\omega = \frac{D}{RT\Delta x \zeta}$$

(7)

(where ζ is the tortuosity and is defined here as the ratio of the actual path length through the membrane to the membrane thickness) and the steady-state relationships $J_s = J_v c_e$, and $c_i = c_e$, into Equation 2. This expression is

$$c_o = -c_i \cdot \frac{J_v \Delta x \zeta (1 + \sigma) + 2Dv}{J_v \Delta x \zeta (\sigma - 1) - 2Dv}$$

(8)

and is suitable for free solution.

6

Under what experimental conditions will sodium chloride precipitate from an initially undersaturated solution when it is passed through a clay membrane? Obviously, the value of c_o must reach or exceed saturation for sodium chloride. We can use Equation 8 to predict what the maximum value of c_o will be for a given set of experimental conditions, and Equation 6 to predict the concentration profile in the CPL in the free solution of the experimental cell.

First, consider an experiment with a clay membrane having a σ of only 0.075. The other experimental parameters are $J_v = 4.88 \times 10^{-5}$ cm/s (which translates to a flow rate of 3 ml/hr through a small, 1 inch diameter experimental cell), $c_i = 6.0$ molar, and $\Delta x = 0.15$cm. Tortuosity = 7.0 (Barone et al. 1990, 1992), D of NaCl = 1.45×10^{-5} cm^2/s, and v = 2. Using Equation 8, we find that $c_o = 6.44$ molar. This is above solubility for sodium chloride ($\approx$6.2 molar) and precipitation should occur at the membrane face in this experiment. The concentration profile in the experimental cell, as calculated from Equation 6, shows that the CPL width is almost 2 cm, and that saturation is exceeded for a distance of approximately 0.22 cm from the membrane (Fig. 2).

One important aspect of these experiments is the effective osmotic pressure ($\sigma\Delta\pi$) because it must be overcome for flow to occur through the membrane. In this experiment, $\sigma\Delta\pi$ equals only 24 psi. This is because the effective osmotic pressure is a function of the difference in solute concentrations on either side of the membrane (See Eqns. 4 and 1) times the reflection coefficient exceeded for a distance of 0.22 cm away from the membrane. Precipitation of NaCl should occur in the portion of the CPL where saturation is reached or exceeded.

If σ is higher than 0.075, then greater pressures will be required to force solution through the membrane. For comparison, let's look at a theoretical experiment in which $\sigma = 0.4$, and $c_i = 5.8$ molar,

with all other parameters remaining the same (Fig. 3). Here we see that the maximum NaCl concentration

reaches 8.5 molar (solubility ≈ 6.2 molar) at the membrane face and that saturation is reached or exceeded
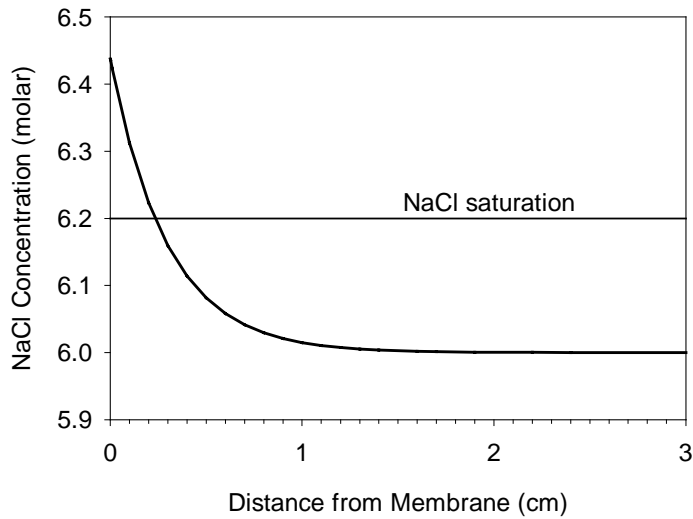
Figure 2. Graph of theoretical results for scenario where $\sigma = 0.075$ for a 6.0 molar NaCl solution
hyperfiltrated through a montmorillonite membrane. Notice that the maximum concentration developed
at the membrane face (c_o) exceeds the saturation value of 6.2 molar and that saturation is reached or
exceeded for a distance of about 0.3 cm away from the membrane.

for a distance of 0.58 cm away from the membrane. The effective osmotic pressure ($\sigma\Delta\pi$) developed in

this experiment is 770 psi. Therefore, even this scenario is achievable for typical reverse osmosis systems

operating at pressures of 1000 to 1200 psi.

Precipitation of sodium chloride at reasonable pressures is dependent upon the membrane having

a sufficiently low osmotic efficiency. How then is this low efficiency assured in the experimental

membranes? Marine and Fritz (1981) derived a model for calculating values of σ by arguing that under

stationary conditions, the thermodynamic forces acting across the membrane are counterbalanced by the

8

sum of mechanical frictional forces operating on the solution components within the membrane. Their

equation is
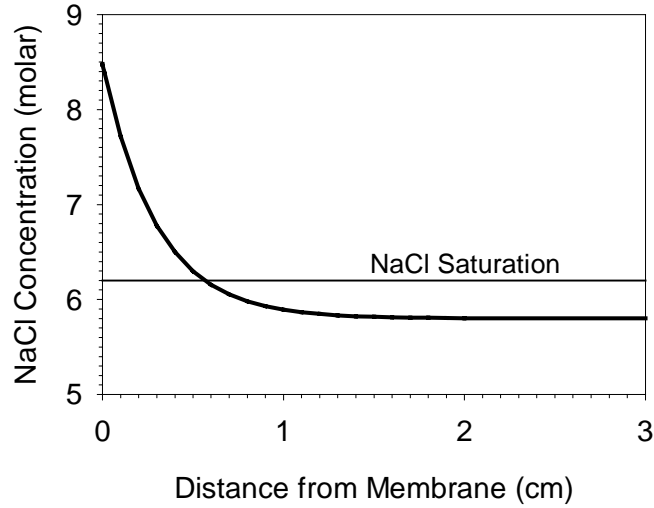
Figure 3. Graph of theoretical results for the second scenario where $\sigma = 0.2$ for a 5.8 molar NaCl solution hyperfiltrated through a montmorillonite membrane. Notice that the maximum concentration developed at the membrane face (c_o) exceeds the saturation value of 6.2 molar and that saturation is reached or exceeded for a distance of 0.58 cm away from the membrane. Precipitation of NaCl should occur in the CPL where saturation is reached or exceeded.

$$\sigma = 1 - \frac{\left[\left(\frac{f_{cw}}{f_{aw}}\right) + 1\right] K_s}{\left\{\left[\left(\frac{f_{cw}}{f_{aw}}\right)\left(\frac{\overline{C}_a}{\overline{C}_c}\right) + 1\right] + \left(\frac{f_{am}}{f_{aw}}\right)\left[\left(\frac{f_{cm}}{f_{am}}\right)\left(\frac{\overline{C}_a}{\overline{C}_c}\right) + 1\right]\right\} \phi_w} \tag{9}$$

where f_{ij} is the frictional coefficient between one mole of component i and an infinite amount of

component j in dyne seconds per centimeter per mole, c refers to the cation, a refers to the anion, w refers

to water, $\overline{C}_i$ is the average concentration of component i across the membrane in dynes per mole, and ϕ_w

refers to the water content of the membrane, which is equivalent to the porosity.

Marine and Fritz (1981) used Equation 9 to model the relationship between porosity and values σ for various NaCl concentrations for montmorillonite membranes (Fig. 4). Their model shows that values of σ between 0.4 and 0.1 should be expected for a 6.0 molar NaCl solution at membrane porosities of between 58 and 73 percent. Previous experiments (Whitworth and DeRosa 1997) suggest that membrane porosities in this range are not easily obtainable by hydraulic compaction during membrane sedimentation alone. Therefore, it will be necessary to physically compact the membranes used in these experiments to the required porosities. Whitworth and Fritz (1994) compacted two montmorillonite membranes to porosities of 44.8 and 62.0 percent using a 20-ton hydraulic press.
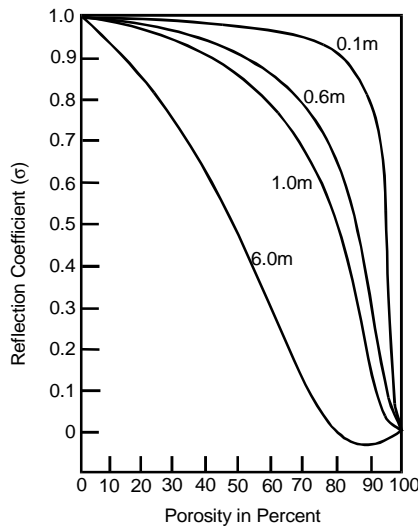
Figure 4. Graph derived from Equation 9 showing relationship between the reflection coefficient and porosity for montmorillonite (smectite) membranes for differing molar concentrations of NaCl (Redrawn from Marine and Fritz 1983). Notice that for 6.0 molar NaCl, porosities between 73% and 58% will yield values of σ of 0.1 and 0.4, respectively.

METHODS

An experimental cell was constructed of 316 stainless steel and was designed to operate at pressures up to 3000 psi (Figure 5). This cell used perforated flow distribution disks in the top of the cell above the solution reservoir and below the 316 stainless steel frit immediately below the membrane to promote uniform flow in the experimental cell.

First undersaturated NaCl solutions were made up. These were made by first mixing a saturated solution of NaCl, filtering with 0.1µm filter paper, and then diluting to the desired saturation level. These solutions were made up immediately before use and stored with almost no head space in a capped container to prevent evaporation.

The clay was prepared by settling in deionized water to achieve the desired particle size, filtering, and then freeze drying to remove all but the bound water. The density of each type of freeze-dried clay used was measured using a pycnometer so that membrane porosity could be calculated from

$$\Phi = \left(1 - \frac{M_c}{\rho_c A \Delta x}\right) \cdot 100 \tag{10}$$

Where Φ is porosity, M_c is the mass of the clay in grams, ρ_c is clay density (g/cm^3), A is membrane area (cm^2), and Δx is membrane thickness (cm). The bentonite we used had a density of 2.17 g/cm^3 and the kaolinite we used had a density of 2.447 g/cm^3.

The clay membranes (either bentonite or kaolinite) were prepared by:

1. Weighing out the desired mass of freeze-dried clay.

2. Placing the clay between filter paper in a steel die. The filter paper/clay sandwich consisted of 1) a layer of Whatman #2 filter paper, 2) a layer of 0.45µm Millipore filter paper, 3) the clay, 4) a layer of 0.45µm Millipore filter paper, and 5) a layer of Whatman #2 filter paper.

3. The clay was then pressed to between 30,000 psi and 50,000 psi in the die in a Carver 20 ton hydraulic press.

4. The resulting membrane sandwich was then removed from the die and placed into the experimental cell.

5. The cell was then assembled.

Following cell assembly, the cell was filled with deionized water and hooked up to the Isco syringe pump (Figure 6). Deionized water was forced through the membrane at a constant flow rate until the pressure reached steady state. The permeability of the membrane to deionized water was then calculated from

$$L_p = \frac{J_{vw}}{\Delta P} \tag{11}$$

Where L_p is the permeability of the membrane to water (cm^3/dyne·s), J_{vw} is the water flux through the membrane in cm^3 per cm^2 of membrane area, and ΔP is the steady-state hydraulic pressure in dynes/cm^2.

Next, the syringe pump was filled with the brine solution after rinsing out the pump three times with the brine solution to remove any remaining deionized water and the brine solution was forced through the experimental cell. The brine solution displaced the deionized water in the cell. Effluent aliquots were collected periodically and saved for analysis. The stock solution was also sampled from the pump and saved for analysis. During the experiment, time, pressure, and flow rate were also recorded each time an effluent sample was taken.

When steady state was reached, or exceeded as desired, as determined from the pressure readings, the syringe pump was stopped. The experimental cell was then disassembled and a sample taken from the solution reservoir. The membrane/filter paper sandwich was then removed and depending on the particular experiment 1) immediately examined under a microscope, 2) any solution remaining on the membrane displaced with acetone or ethanol, and then examined under a light microscope or with an electron microprobe, except in the case of experiment 4 where the membrane was quickly (less than 10 minutes total elapsed time) examined under ¼ inch of brine solution from the cell.

In four of the experiments, a light-weight cooking oil was pumped through the experimental cell to displace any remaining brine solution. These membranes were then removed from the experimental cell, dried, and examined with the ion microprobe. The microprobe used was a CAMECA SX-100 electron microprobe equipped with one energy-dispersive and three wave-length-dispersive spectrometers. It resides in the NMBMMR microprobe laboratory.
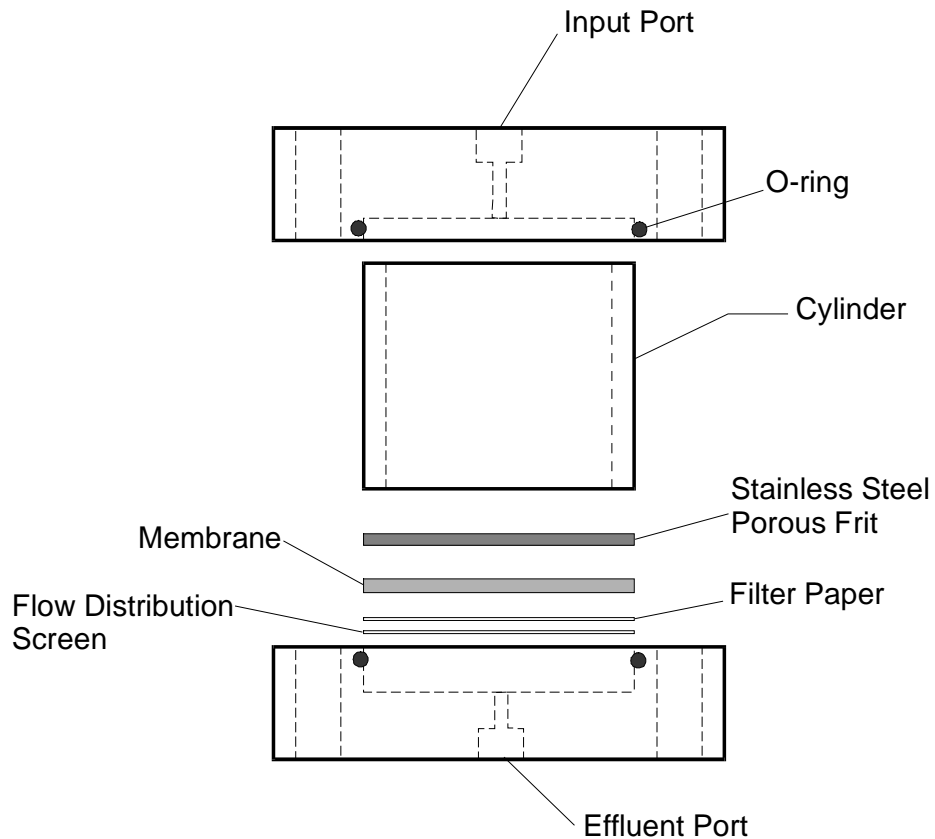
Figure 5. Experimental cell for precipitation experiments. The entire assembly is locked in place with nuts on threaded rods which pass through the holes near the edges of the top and bottom plates. Since all cell dimensions are known to ± 0.001 inches, the membrane thickness can be calculated from the measured distance between the inside surfaces of the outer plates. Cylinders of differing lengths can be used depending upon CPL length for a given experiment.
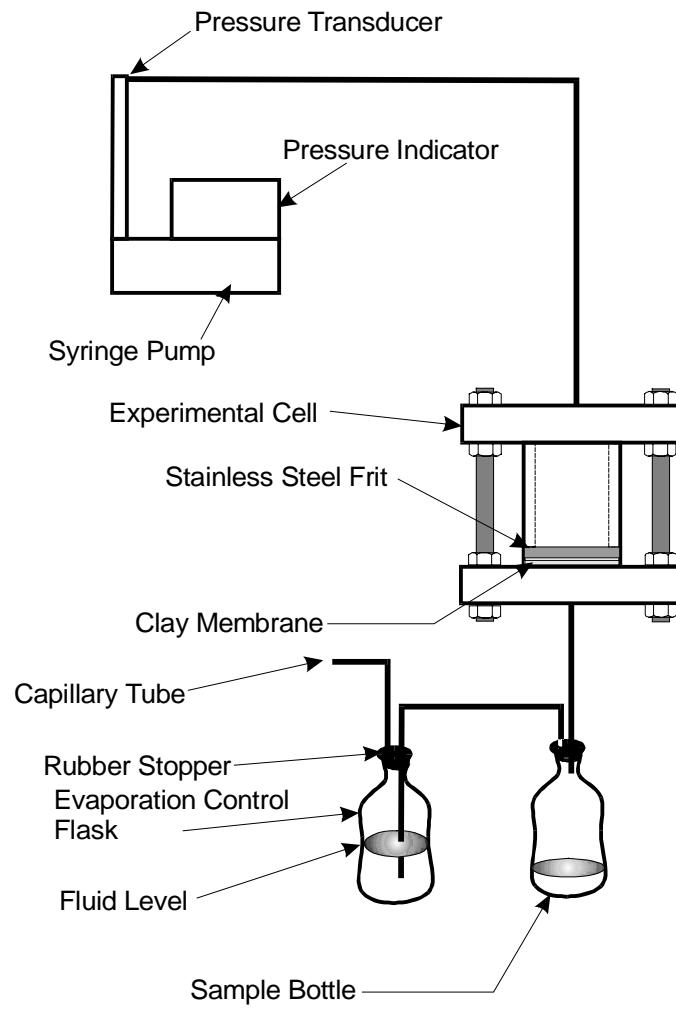
Figure 6. Experimental setup for hyperfiltration experiments.

RESULTS

Fourteen experiments were started, but only seven experiments are reported here. The unreported experiments were either aborted due to pump or other failures, or, in one case, performed with a synthetic membrane with no discernable results.

Experiment 4 (Table 1) used a kaolinite clay membrane compacted to 50,000 psi. This membrane was at 71.8 percent porosity. The membrane was examined at the end of the experiment under a microscope but, while several crystals were present, none were identifiable as sodium chloride crystals. The brine was displaced with acetone before microscopic examination.

Table 1. Results for Experiment 4.

Sample Number	Δp (psi)	Cl- (moles/L)	Jv (cm/s)	Elapsed Time (hrs)	Comments
RC4-0	--	4.66	--	--	Stock Solution
RC4-1	370	2.85	3.29×10^{-4}	1.87	--
RC4-2	510	3.76	3.29×10^{-4}	6.50	--
RC4-3	535	4.31	3.29×10^{-4}	7.65	--
RC4-4	620	--	3.29×10^{-4}	17.32	--
RC4-5	670	4.45	3.29×10^{-4}	30.15	--
RC4-6	700	4.70	3.29×10^{-4}	39.38	--
RC4-7	715	4.59	3.29×10^{-4}	44.15	--
RC4-8	720	4.83	3.29×10^{-4}	51.02	--
RC4-9	760	4.65	3.29×10^{-4}	63.20	--
RC4-10	770	4.71	3.29×10^{-4}	66.80	--

Experiment 7 (Table 2) used a kaolinite membrane compacted to 50,000 psi. The porosity of this membrane was 63.3 percent. At the end of this experiment, the membrane was removed from the cell and immediately examined while still submersed in the brine solution. Figure 7 is a photograph of a crystal thought to be NaCl taken with a light microscope. This crystal, and others, were visible by the naked eye on the surface of the membrane when it was first removed from the experimental cell.

Table 2. Results for Experiment 7.

Sample Number	Δp (psi)	Cl- (moles/L)	Jv (cm/s)	Elapsed Time (hrs)	Comments
RC7-0	--	4.64	--	--	Stock Solution
RC7-1	763	0.60	1.37×10^{-3}	0.33	
RC7-2	939	2.04	1.64×10^{-3}	0.80	
RC7-3	1097	3.21	1.64×10^{-3}	1.30	
RC7-4	1204	3.84	1.64×10^{-3}	1.80	
RC7-5	1277	4.16	1.64×10^{-3}	2.30	
RC7-6	1327	4.37	1.64×10^{-3}	2.80	
RC7-7	1363	4.47	1.64×10^{-3}	3.30	
RC7-8	1385	4.54	1.64×10^{-3}	3.80	
RC7-9	1405	4.57	1.64×10^{-3}	4.52	
RC7-10	1418	4.58	1.64×10^{-3}	5.52	
RC7-11	1430	4.59	1.64×10^{-3}	6.52	
RC7-12	1442	4.63	1.64×10^{-3}	7.64	
RC7-13	1457	4.64	1.64×10^{-3}	10.76	
RC7-14	1479	4.68	1.64×10^{-3}	12.96	
RC7-15	1439	4.68	1.64×10^{-3}	22.49	
RC7-16	1450	4.72	1.64×10^{-3}	25.72	
RC7-17	--	4.74	1.64×10^{-3}	--	
RC7-18	1245	4.70	1.64×10^{-3}	34.19	
RC7-19	1259	4.68	1.64×10^{-3}	46.37	
RC7-20	1189	4.65	1.64×10^{-3}	50.92	
RC7-21	--	4.67	1.64×10^{-3}	57.49	
RC7-22	1166	4.66	1.64×10^{-3}	60.09	
RC7-23	--	4.55	--	--	Cell Solution
RC7-24	--	4.64	--	--	Pump Solution

Figure 7. Microphotograph of crystal observed on kaolinite membrane at conclusion of Experiment 7. The size of this crystal is about 0.025 mm by 0.0275 mm and the total magnification is 2000X.

Experiment 8 (Table 3) used a kaolinite membrane compacted to 50,000 psi.   The porosity of this membrane was 72.7 percent. At the end of the experiment, the membrane was removed from the experimental cell, washed free of brine using ethanol via the method of Fritz and Eady (1985) and then examined on the microprobe. Figures 8 and 9 show the results of this examination. To test if the ethanol might precipitate NaCl, we poured some ethanol into a small beaker half filled with brine. There was an

immediate cloud of white precipitate that we confirmed was NaCl. Therefore, the results of this

experiment are inconclusive. We stopped using ethanol to displace brine after this experiment.

Table 3. Results for Experiment 8.

Sample Number	Δp (psi)	Cl- (moles/L)	Jv (cm/s)	Elapsed Time (hrs)	Comments
RC8-0	--	4.55	--	--	Stock Solution
RC8-1	539	0.25	8.77×10^{-4}	0.33	--
RC8-2	577	1.00	8.77×10^{-4}	0.83	--
RC8-3	632	1.74	8.77×10^{-4}	1.36	--
RC8-4	687	2.58	8.77×10^{-4}	1.93	--
RC8-5	730	3.22	8.77×10^{-4}	2.43	--
RC8-6	760	3.62	8.77×10^{-4}	2.93	--
RC8-7	787	3.91	8.77×10^{-4}	3.46	--
RC8-8	803	4.10	8.77×10^{-4}	3.96	--
RC8-9	817	4.19	8.77×10^{-4}	4.49	--
RC8-10	828	4.32	8.77×10^{-4}	5.02	--
RC8-11	857	4.46	8.77×10^{-4}	5.90	--
RC8-12	862	4.48	8.77×10^{-4}	7.12	--
RC8-13	872	4.50	8.77×10^{-4}	11.97	--
RC8-14	864	4.56	8.77×10^{-4}	19.47	--
RC8-15	866	4.51	8.77×10^{-4}	22.5	--
RC8-16	773	4.55	8.77×10^{-4}	25.38	--
RC8-17	709	4.54	8.77×10^{-4}	29.96	--
RC8-18	746	5.09	8.77×10^{-4}	34.44	--
RC8-19	793	4.56	8.77×10^{-4}	42.64	--
RC8-20	801	4.56	8.77×10^{-4}	46.22	--
RC8-21	804	4.58	8.77×10^{-4}	52.70	--
RC8-22	--	4.57	8.77×10^{-4}	58.18	--
RC8-23	762	4.56	8.77×10^{-4}	66.28	--
RC8-24	764	4.56	8.77×10^{-4}	71.25	--
RC8-25	767	4.59	8.77×10^{-4}	75.55	--
RC8-26	753	4.58	8.77×10^{-4}	79.80	--
RC8-27	712	4.59	8.77×10^{-4}	90.48	--
RC8-28	--	4.58	--	--	Pump Solution
RC8-29	--	4.53	--	--	Cell Solution
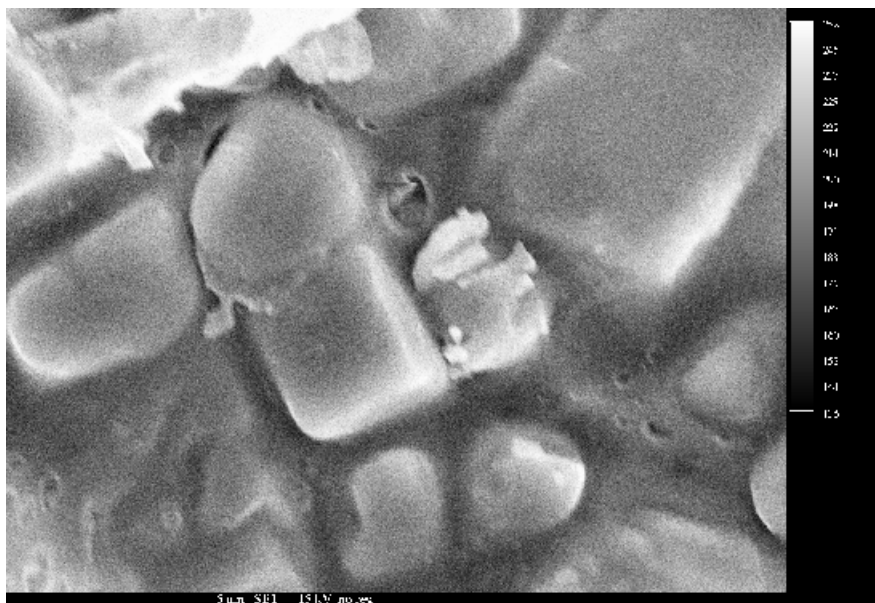
Figure 8. Electron micrograph of a NaCl crystal present on the surface of the filter paper above the membrane of Experiment 8. These crystals are thought to have formed by precipitation due to addition of ethanol. We discovered that this published technique (Fritz and Eady 1985) is not suitable for use with brines. The ethanol forms an azeotrope with the brine resulting in NaCl precipitation.

Figure 9. Energy dispersive X-ray scan of crystals shown in Figure 8. The peaks in this scan confirm that the crystals are composed of NaCl.

Experiment 11 (Table 4) used a bentonite membrane compacted to 30,000 psi. The porosity of this membrane was 32.2 percent. To avoid the problems of possible NaCl precipitation by displacing the brine with ethanol, we used light-weight cooking oil to displace the brine from the experimental cell at the end of the experiment. No crystals formed in our beaker tests when we poured brine into the oil or oil into the brine. After examination with the microprobe, we saw numerous NaCl crystals on the membrane (Figures 10, 11, and 12). These are interpreted to have formed due to membrane-enhanced concentration on the high pressure side of the membrane.

Table 4. Results for Experiment 11.

Sample Number	Δp (psi)	Cl- (moles/L)	Jv (cm/s)	Elapsed Time (hrs)	Comments
RC11-0	--	4.56	--	--	Stock Solution
RC11-1	937	0.45	1.10×10^{-5}	27.0	--
RC11-2	1098	0.96	1.10×10^{-5}	56.5	--
RC11-3	1138	1.56	1.10×10^{-5}	94.0	--
RC11-4	1203	2.19	1.10×10^{-5}	118.3	--
RC11-5	--	2.68	--	--	--
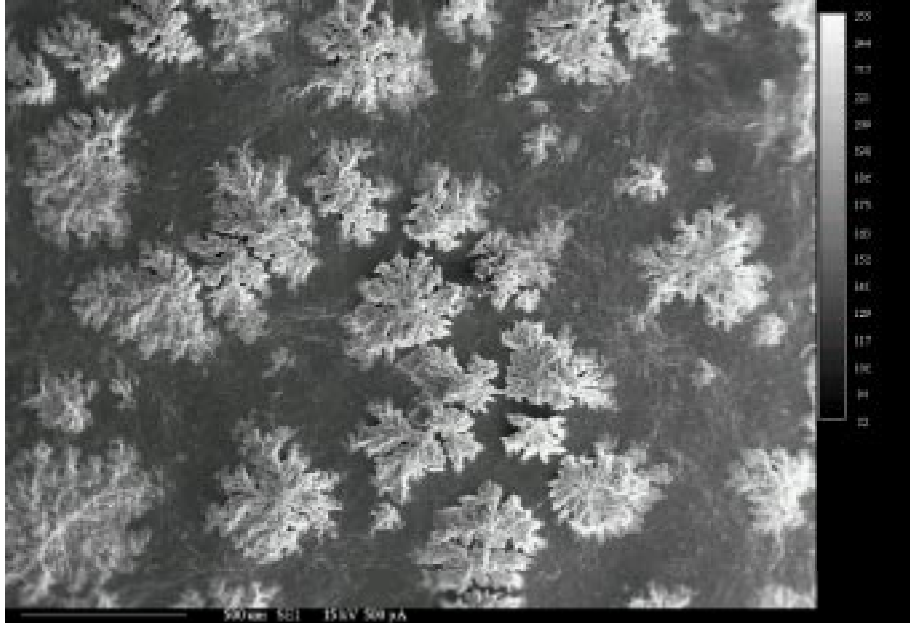
Figure 10. Electron micrograph of NaCl crystals present on the surface of the membrane of Experiment 11. These were identified using energy dispersive X-ray scans as being NaCl. The brine remaining in the experimental cell was displaced with light weight cooking oil before the cell was disassembled. Beaker tests demonstrated that the cooking oil does not precipitate NaCl.

Figure 11. Enlargement of a single crystal cluster from Experiment 11 shown in Figure 10.
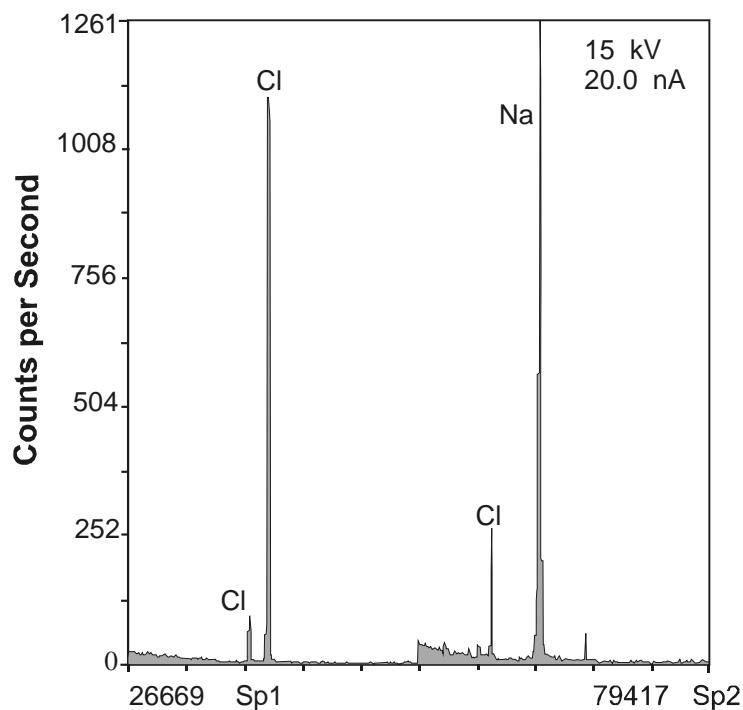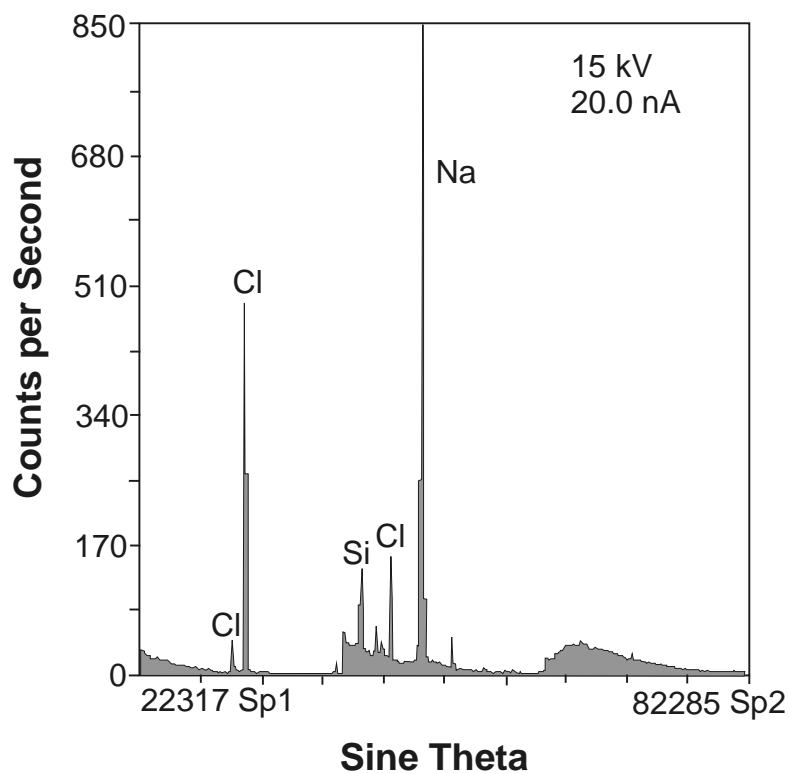
Figure 12. Energy dispersive X-ray scan of crystals shown in Figures 10 and 11. The peaks in this scan confirm that the crystals shown in Figures 10 and 11 are composed of NaCl.

Experiment 12 (Table 5) used a kaolinite membrane compacted to 50,000 psi. It had a porosity of 30.5 percent. At the end of this experiment the brine remaining in the experimental cell was displaced with lightweight cooking oil. Subsequent examination on the microprobe showed the presence of NaCl crystals (Figures 13 and 14). These crystals were interpreted to have formed due to membrane enhanced concentration on the high pressure side of the membrane.

Table 5. Results for Experiment 12.

Sample Number	Δp (psi)	Cl- (moles/L)	Jv (cm/s)	Elapsed Time (hrs)	Comments
RC12-0	--	4.63	1.10×10^{-3}	--	Stock Solution
RC12-1	346	0.32	1.10×10^{-3}	0.27	--
RC12-2	377	1.10	1.10×10^{-3}	0.57	--
RC12-3	422	1.87	1.10×10^{-3}	1.02	--
RC12-4	466	2.79	1.10×10^{-3}	1.55	--
RC12-5	508	3.42	1.10×10^{-3}	2.22	--
RC12-6	555	4.02	1.10×10^{-3}	3.78	--
RC12-7	563	4.35	1.10×10^{-3}	4.23	--
RC12-8	573	4.44	1.10×10^{-3}	5.23	--
RC12-9	583	4.46	1.10×10^{-3}	6.75	--
RC13-10	583	4.52	1.10×10^{-3}	9.52	--
RC12-11	579	4.51	1.10×10^{-3}	11.8	--
RC12-12	589	4.54	1.10×10^{-3}	24.4	--
RC12-13	--	4.54	1.10×10^{-3}	29.5	--
RC12-14	543	4.52	1.10×10^{-3}	33.0	--
RC12-15	541	4.52	1.10×10^{-3}	36.0	--
RC12-16	552	4.57	1.10×10^{-3}	47.2	--
RC12-17	534	4.54	1.10×10^{-3}	53.0	--
RC12-18	535	4.62	1.10×10^{-3}	58.1	--
RC12-19	542	4.59	1.10×10^{-3}	69.7	--
RC12-20	542	4.58	1.10×10^{-3}	71.6	--
RC12-21	531	4.58	1.10×10^{-3}	75.3	--
RC12-22	531	4.58	1.10×10^{-3}	81.7	--
RC12-23	539	4.59	1.10×10^{-3}	94.5	--
RC12-24	530	4.59	1.10×10^{-3}	100.8	--
RC12-25	524	4.52	1.10×10^{-3}	105.8	--
RC12-26	540	4.66	1.10×10^{-3}	118.1	--
RC12-27	543	4.65	1.10×10^{-3}	123.0	--
RC12-28	--	4.59	--	--	Pump Solution
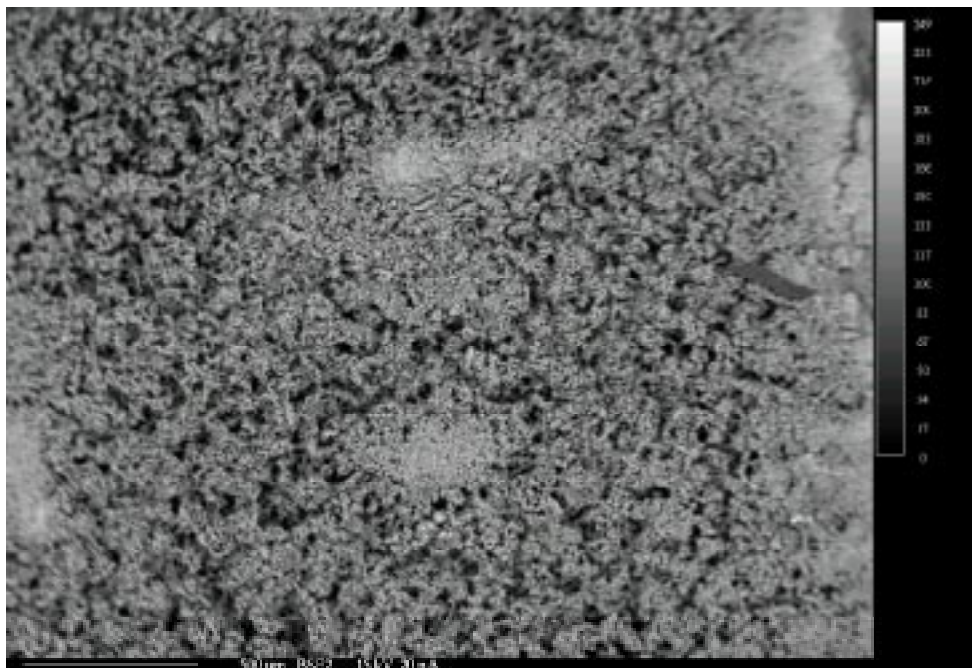
Figure 13. Microprobe scan showing distribution of NaCl crystals across surface of kaolinite membrane from Experiment 12. The NaCl is the bright white part of the scan. The brine remaining in the experimental cell was displaced with light weight cooking oil before the cell was disassembled. Beaker tests demonstrated that the cooking oil does not precipitate NaCl.
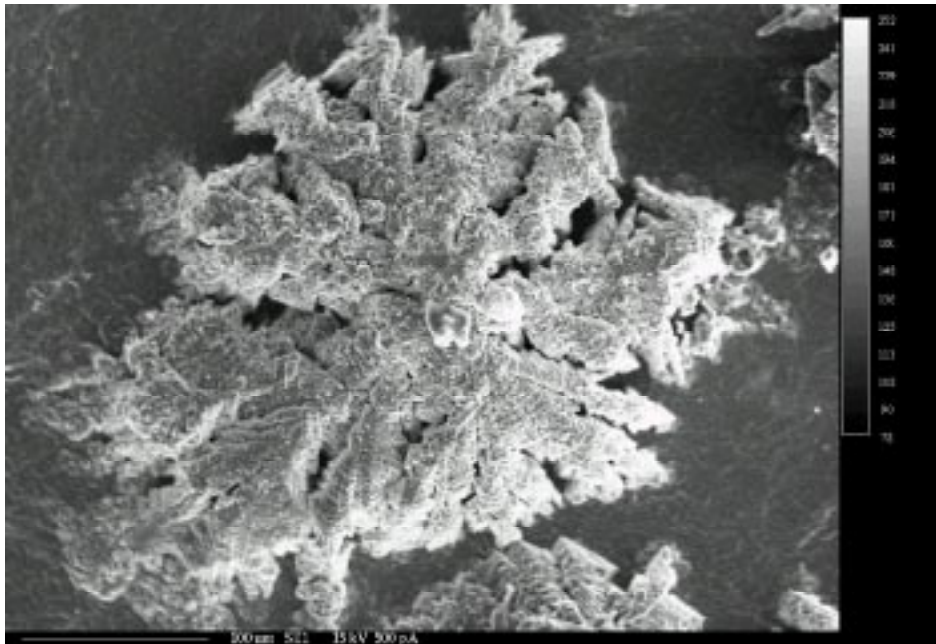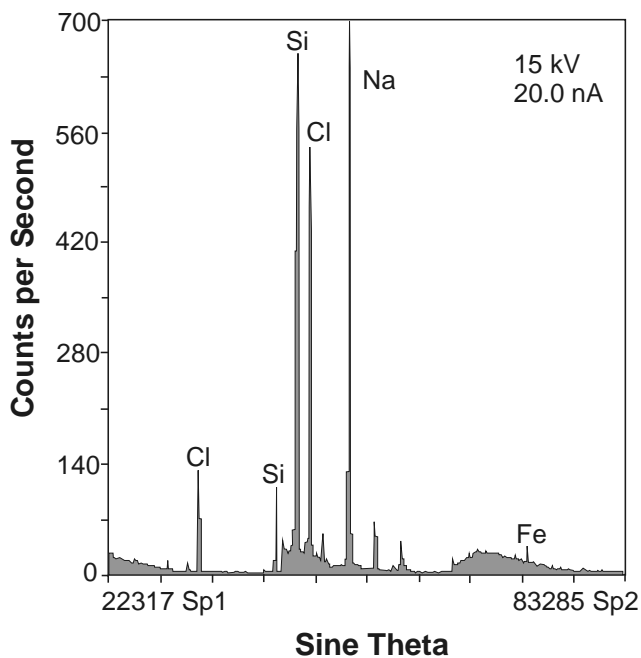

Figure 14. Energy dispersive X-ray scan of crystals shown in Figure 13. The peaks in this scan confirm that the crystals are composed of NaCl. This scan is of the white area in Figure 13.

Experiment 13 (Table 6) used a kaolinite membrane compacted to 50,000 psi. The porosity of this membrane was 37.1 percent. Again, at the end of the experiment, the brine remaining in the experimental cell was displaced with lightweight cooking oil. The membrane was then examined on the microprobe. Figures 15 and 16 show examples of the crystals observed. These crystals are interpreted to have formed due to membrane-enhanced concentration on the high pressure side of the membrane.

Table 6. Results for Experiment 13.

| Sample Number	Δp (psi)	Cl- (moles/L)	Jv (cm/s)	Elapsed Time (hrs)	Comments
RC13-0	--	4.82	--	--	Stock Solution
RC13-1	572	0.68	9.86×10^{-4}	0.35	--
RC13-2	612	1.16	9.86×10^{-4}	0.67	--
RC13-3	668	1.74	9.86×10^{-4}	1.02	--
RC13-4	724	2.36	9.86×10^{-4}	1.35	--
RC13-5	777	2.87	9.86×10^{-4}	1.70	--
RC13-6	823	3.29	9.86×10^{-4}	2.03	--
RC13-7	862	3.61	9.86×10^{-4}	2.37	--
RC13-8	901	3.86	9.86×10^{-4}	2.70	--
RC13-9	931	4.15	9.86×10^{-4}	3.03	--
RC13-10	971	4.26	9.86×10^{-4}	3.65	--
RC13-11	1006	4.30	9.86×10^{-4}	4.23	--
RC13-12	1031	4.56	9.86×10^{-4}	4.73	--
RC13-13	1068	4.61	9.86×10^{-4}	5.58	--
RC13-14	1082	4.76	9.86×10^{-4}	6.75	--
RC13-15	1099	4.81	9.86×10^{-4}	8.42	--
RC13-16	1107	4.79	9.86×10^{-4}	11.48	--
RC13-17	1128	4.73	9.86×10^{-4}	20.77	--
RC13-18	1134	4.80	9.86×10^{-4}	25.48	--
RC13-19	1053	4.72	9.86×10^{-4}	29.87	--
RC13-20	1076	4.81	9.86×10^{-4}	34.50	--
RC13-21	1072	4.77	9.86×10^{-4}	45.33	--
RC13-22	1076	4.71	9.86×10^{-4}	51.95	--
RC13-23	1055	4.78	9.86×10^{-4}	57.83	--
RC13-24	1042	4.81	9.86×10^{-4}	69.03	--
RC13-25	1055	4.37	9.86×10^{-4}	79.15	--
RC13-26	1031	4.88	9.86×10^{-4}	94.93	--
RC13-27	1009	4.79	9.86×10^{-4}	100.37	--
RC13-28	--	4.81	--	--	Pump Solution
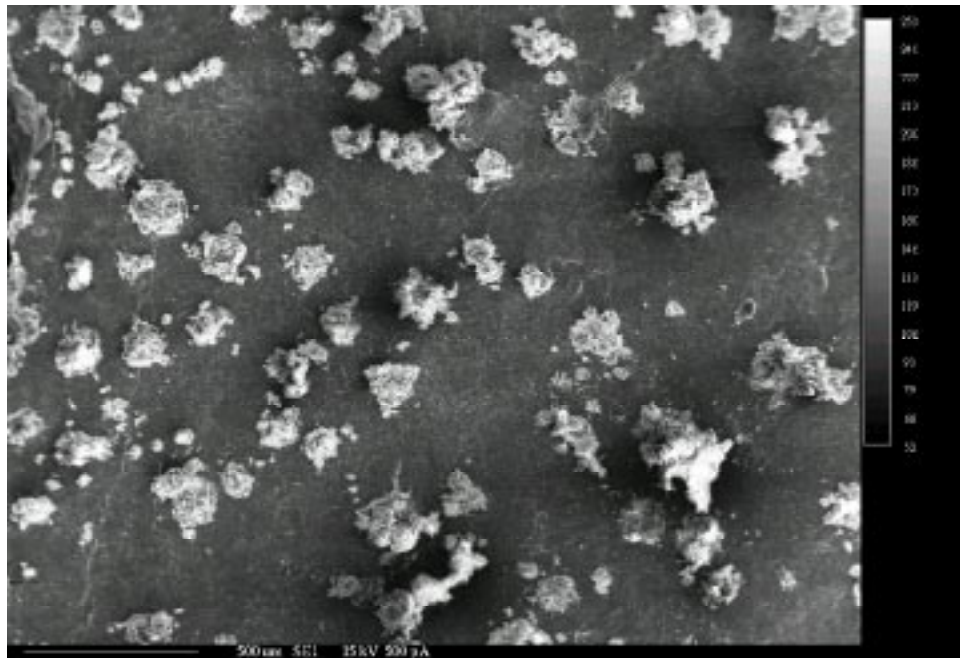
Figure 15. Microprobe scan showing distribution of NaCl crystals across surface of kaolinite membrane from Experiment 13. The brine remaining in the experimental cell was displaced with light weight cooking oil before the cell was disassembled. Beaker tests demonstrated that the cooking oil does not precipitate NaCl.
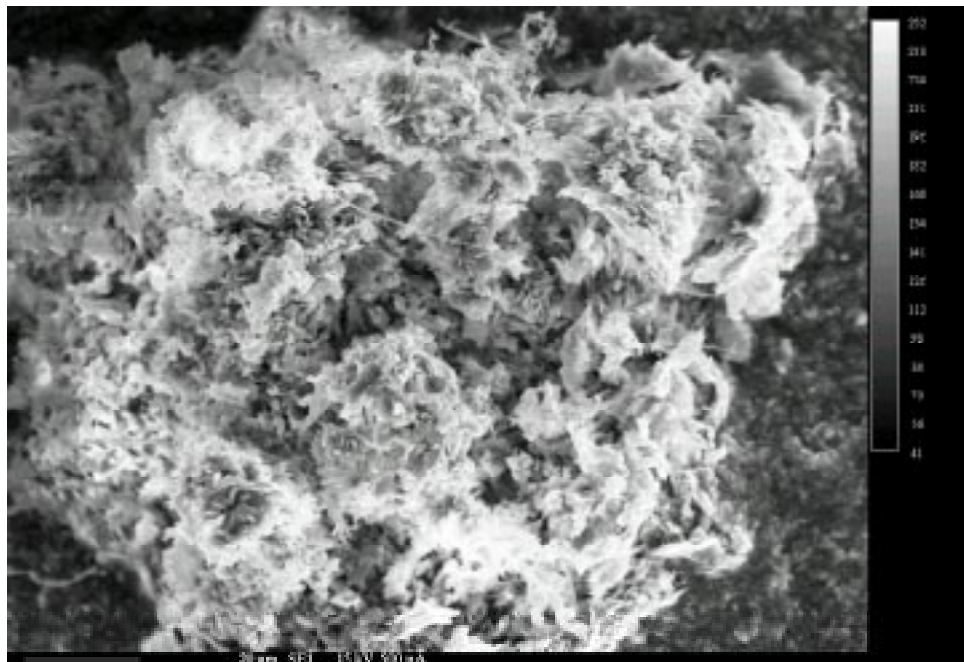
Figure 16. Close-up of one of the crystal clusters shown in Figure 15.
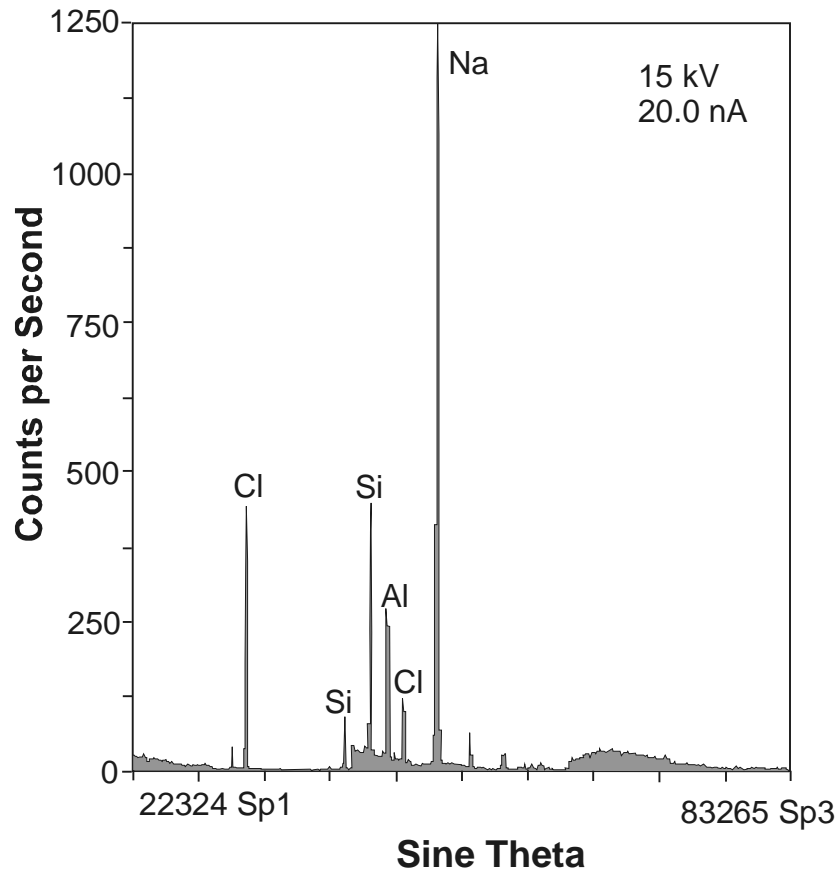
Figure 17. Energy dispersive X-ray scan of crystals shown in Figures 15 and 16. The peaks in this scan confirm that the crystals are composed of NaCl.

Experiment 14 (Table 7) used a bentonite membrane compacted to 30,000 psi. The porosity of this membrane was 44.0 percent. At the end of the experiment, the brine remaining in the experimental cell was displaced with light weight cooking oil. The membrane was then examined on the microprobe. No NaCl crystals were observed when this membrane was examined on the microprobe. However, Figure 18 shows some unidentified crystals that were observed.

Table 7. Results for Experiment 14.

Sample Number	Δp (psi)	Cl- (mg/cm^3)	Jv (cm/s)	Elapsed Time (hrs)	Comments
RC14-0	--	4.90	--	--	Stock Solution
RC14-1	130	0.52	1.10×10^{-4}	2.17	--
RC14-2	388	0.90	1.64×10^{-4}	4.08	--
RC14-3	429	1.55	1.64×10^{-4}	6.37	--
RC14-4	488	2.40	1.64×10^{-4}	10.05	--
RC14-5	601	3.77	1.64×10^{-4}	22.03	--
RC14-6	615	4.44	1.64×10^{-4}	24.57	--
RC14-7	640	4.63	1.64×10^{-4}	33.75	--
RC14-8	639	4.79	1.64×10^{-4}	47.67	--
RC14-9	678	4.85	1.64×10^{-4}	68.25	--
RC14-10	748	4.94	1.64×10^{-4}	92.88	--
RC14-11	790	4.92	1.64×10^{-4}	118.50	--
RC14-12	785	4.85	1.64×10^{-4}	139.63	--
RC14-13	795	4.83	1.64×10^{-4}	166.00	--

Figure 18. Electron micrograph of unknown crystals on surface of membrane from Experiment 14. These crystals do not have the habit of NaCl crystals. No energy dispersive X-ray scan is available for these crystals. Their composition is unknown. No similar crystals were observed on any of the other membranes.

Before discussing the results, it is necessary to calculate the membrane coefficients for each of the experiments. Whitworth and DeRosa (1997) derived a steady-state solution for σ that does not use the measured values for c_e. This can be done, because at steady-state $c_e = c_i$. Therefore, by substituting Equation 4 into Equation 1 we obtain

$$J_v = L_P(\Delta P - \sigma v RT(c_o - c_e))$$ (12)

which since $c_e = c_i$ at steady-state is the equivalent of

$$J_v = L_P(\Delta P - \sigma v RT(c_o - c_i))$$ (13)

Fritz and Marine (1983) stated that

$$\omega = \frac{D}{RT\Delta x\zeta} \tag{14}$$

where ζ is the tortuosity of the flow path through the membrane defined by the ratio of the actual length divided by the membrane thickness. By substituting Equation 4, Equation 13, and the steady-state relationship $J_S = J_v c_e$ into Equation 2 we obtain

$$J_v \cdot c_i = \frac{c_o + c_i}{2}(1-\sigma)J_v + \frac{D}{RT\Delta x\zeta}vRT(c_o - c_i) \tag{15}$$

Solving equations 12 and 14 for σ and setting them equal we obtain

$$\frac{L_P\Delta P - J_v}{L_P vRT(c_o - c_i)} = \frac{\dfrac{2Dv(c_o - c_i)}{\Delta x\zeta} - J_v(c_i - c_o)}{J_v(c_0 + c_i)} \tag{16}$$

Solving this equation for c_i yields a polynomial solution with two roots, one positive and one negative root.

$$\text{root1} = \frac{1}{2L_P vRT(J_v\Delta x - 2vD)} \cdot (-2L_P vRTJ_v c_i\Delta x\zeta - 4L_P v^2 RTDc_i + \Delta x\zeta J_v L_P\Delta P +$$
$$\Delta x^{1/2}\zeta^{1/2}(-8\zeta\Delta xc_i J_v^3 TRvL_P + 8\zeta\Delta xc_i J_v^2 TRvL_P^2 + \zeta\Delta xJ_v^4 - 2\zeta\Delta x\Delta PL_P J_v^3 + \tag{17}$$
$$\zeta\Delta x\Delta P^2 L_P^2 J_v^2 - 16J_v^2 c_i DTRv^2 L_P^2)^{1/2}$$

Table 8. Experimental results and calculated membrane coefficients.

Experiment	Δx (cm)	Mc (g)	Clay Type	ϕ (%)	Hydraulic Pressure (psi)	J_{vw} (cm/s) (x 10^{-4})	ΔP_w (psi)	J_v (cm/s) (x 10^{-4})	ΔP (PSI)	C_i (moles/L)	C_o (moles/L)	σ unitless	ω (x 10^{-15}) (mole/dyne·s)	L_p (x 10^{-12}) (cm^3/dyne·s)	NaCl Precipitation Observed
4	0.0445	0.35	K	71.8	50,000	5.34	1020	3.29	770	4.66	5.80	0.18	2.0	7.60	No
7	0.0518	0.53	K	63.3	50,000	21.6	1000	16.4	1166	4.64	7.08	0.23	1.7	31.3	Yes-- Visual/light microscope
8	0.0695	0.53	K	72.7	50,000	8.77	539	8.77	712	4.55	6.04	0.16	1.3	23.6	No
11	0.0083	0.1392	B	32.2	30,000	0.159	1200	0.11	1203	4.56	--	--	--	0.19	Yes-- Microprobe
12	0.0257	0.4985	K	30.5	50,000	18.6	600	10.95	543	4.64	6.11	0.18	3.5	45.6	Yes-- Microprobe
13	0.0285	0.4999	K	37.1	50,000	10.8	700	9.86	1009	4.82	6.98	0.24	3.2	22.5	Yes-- Microprobe
14	0.0095	0.1483	B	44.0	30,000	2.66	1000	1.64	795	4.90	5.52	0.40	9.5	3.85	No

Note: M_c is mass of freeze-dried clay, K is kaolinite, B is bentonite, J_{vw} is flux of deionized water through membrane, ΔP_w is hydraulic pressure at steady state for run with deionized water. Values of σ, ω, and c_o are calculated using the method of Whitworth and DeRosa (1997). To convert psi to dynes/cm^2 multiply by 68947.57.

$$\text{root2} = \frac{1}{2L_P vRT(J_v \Delta x - 2vD)} \cdot (-2L_P vRTJ_v c_i \Delta x \zeta - 4L_P v^2 RTDc_i + \Delta x \zeta J_v L_P \Delta P -$$
$$\Delta x^{1/2} \zeta^{1/2} (-8\zeta \Delta x c_i J_v^3 TRvL_P + 8\zeta \Delta x c_i J_v^2 TRvL_P^2 + \zeta \Delta x J_v^4 - 2\zeta \Delta x \Delta P L_P J_v^3 + \quad\quad (18)$$
$$\zeta \Delta x \Delta P^2 L_P^2 J_v^2 - 16J_v^2 c_i DTRv^2 L_P^2)^{1/2}$$

Since negative values of σ have no meaning, the positive root (root 2) is chosen to calculate c_o. The reflection coefficient is then calculated from

$$\sigma = \frac{-(J_v - L_p \Delta P)}{(L_p vRTc_o - L_p vRTc_i)} \quad\quad (19)$$

The membrane coefficients σ, ω and c_o were calculated (Table 8) for each of the seven experiments using the approach of Whitworth and DeRosa (1997). Table 8 is a summary table and contains values of the measured experimental parameters as well as the calculated steady-state values of the membrane coefficients. The data in Table 8 is the basis for the discussion of the results that follows.

DISCUSSION

We see from Table 8 that when the calculated values of c_o are above solubility for NaCl (about 6.2M) that precipitation was observed. Except in one case, Experiment 12, no NaCl precipitate was observed when the calculated value of c_o was below the solubility for NaCl. However, the calculated value of c_o of 6.11M is fairly close to the solubility of 6.2M. This discrepancy may be due to error either in the measurement of the experimental values and/or error in the model itself. In general, however, the model seems to predict the NaCl precipitation fairly well.

No calculated values of the membrane coefficients are shown for Experiment 11 because the calculated values made no physical sense. This is attributed to a probable error in experimental measurement of L_p.

Much of the clay membrane literature implies that kaolinite, because it is essentially uncharged, is never as efficient a membrane as is bentonite, montmorillonite, or smectite which have significant negative charges on the crystalline lattice (Fritz and Marine 1983). Fritz (1986) states that most of the ion

rejection capability of clays occurs because the negatively charged electrical field in the clay pore (the double layer) repels the anion. This is commonly called anion rejection. Surprisingly, hyperfiltration of undersaturated NaCl brine solutions through kaolinite resulted in more frequent NaCl precipitation than did hyperfiltration through bentonite. Only one experiment using bentonite resulted in NaCl precipitation, but three experiments using kaolinite precipitated NaCl. This suggests that, especially for concentrated solutions, that solute separation is most likely a function of the relative size of the solute and the pore size of the clay. The electric charge of the clay appears to be a secondary separation mechanism at best for brines. This is a reasonable and expected conclusion, because at concentrations above one molar, the electrical double layer is thought to completely collapse.

Examination of Tables 2, 6, and 7 show that the analytical precision of NaCl analyses masks any effluent concentration decreases due to NaCl precipitation. The analytical precision of these analyses is generally estimated at $\pm 3\%$ at two standard deviations including dilution errors.

Work is continuing on developing commercial applications of membrane-induced precipitation at the Petroleum Recovery Research Center at New Mexico Tech and is funded by the National Petroleum Technology Office of the Department of Energy.

SUMMARY AND CONCLUSIONS

A series of seven experiments is reported here where undersaturated NaCl solutions were passed through clay membranes. Most of these solutions were approximately 90% saturated. NaCl crystals were observed on the membranes for several experiments and X-ray dispersive scans during examination with the microprobe. While the experiments demonstrated the validity of the proposed process, development of commercial applications will take further work. Work is continuing on developing commercial applications at the Petroleum Recovery Research Center at New Mexico Tech and this project continuation is funded by the National Petroleum Technology Office of the Department of Energy.

REFERENCES CITED

Barone, F. S.; Rowe, R. K.; and Quigley, R. M. 1992. Estimation of chloride diffusion coefficient and tortuosity factor for mudstone. Journal of Geotechnical Engineering. 118: 1031-1047.

Barone, F. S.; Rowe, R. K.; and Quigley, R. M. 1990. Laboratory determination of chloride diffusion coefficient in intact shale. Canadian Geotechnical Journal. 27: 177-184.

Elrick, D. E., D. E. Smiles, N. Baumgartner, and P. H. Groenvelt. 1976. Coupling phenomena in saturated homo-ionic montmorillonite: I. Experimental. Soil Science Society of America Journal. 40:490-491.

Feth, J. H. 1970. Saline groundwater resources of the conterminous United States. *Water Resources Research*, 6: 1454-1457.

Fetter, C. W. 1988. Applied Hydrogeology. Merrill, Columbus Ohio. 592 p.

Fritz, S. J. and T. M. Whitworth. 1994. Hyperfiltration-induced fractionation of lithium isotopes: ramifications relating to representativeness of aquifer sampling. Water Resources Research. 30:225-235.

Fritz, S. J. and C. D. Eady. 1985. Hyperfiltration-induced precipitation of calcite. Geochimica et Cosmochimica Acta. 49:761-768.

Fritz, S. J. 1986. Ideality of clay membranes in osmotic processes: a review. Clays and Clay Minerals. 34:214-223.

Fritz, S. J. and I. W. Marine. 1983. Experimental support for a predictive osmotic model of clay membranes. Geochimica et Cosmochimica Acta. 47:1515-1522.

Harris, F. L., G. B. Humphreys, and K. S. Spiegler. 1976. Reverse osmosis (hyperfiltration) in water desalination. In P. Meares, ed., Membrane Separation Processes. Elsevier, Amsterdam, Chapter 4.

Hood, J. W. and L. R. Kister. 1962. Saline-water resources of New Mexico, U.S. Geological Survey Water-Supply Paper 1601. 70 p.

Katchalsky, A. and P. F.Curran. 1965. Biophysic*s*. Harvard University Press, Cambridge. 248 p.

Kedem, O. and A. Katchalsky. 1962. A physical interpretation of the phenomenological coefficients of membrane permeability. Journal of General Physiology. 45:143-179.

Mariñas, B. J. and R. E. Selleck. 1992. Reverse osmosis treatment of multicomponent electrolyte solutions. Journal of Membrane Science. 72:211-229.

Marine, I. W., and S. J. Fritz. 1981, Osmotic model to explain anomalous hydraulic heads, Water Resources Research, 17: 73-82.

Spiegler, K. S. and O. Kedem. 1966. Thermodynamics of hyperfiltration (reverse osmosis): criteria for efficient membranes. Desalination. 1:311-326.

Whitworth, T. M., B. J. Mariñas, and S. J. Fritz. 1994. Isotopic fractionation and overall permeation of lithium by a thin-film composite polyamide reverse osmosis membrane. Journal of Membrane Science. 88:231-241.

Whitworth, T. M. and G. DeRosa. 1997. Geologic membrane controls on saturated zone heavy metal transport. New Mexico Water Resources Research Institute Report No. 303, Las Cruces, New Mexico, 88 p.

Whitworth, T. M. and S. J. Fritz. 1994. Electrolyte-induced solute permeability effects in compacted smectite membranes. Applied Geochemistry. 9:533-546.